ESD-TR-69-111

Technical Note

1969-28

E. Gehrels

Interferometric Phase and Amplitude Fluctuation Measurements Over a 7-km Atmospheric Path

13 May 1969

Prepared for the Advanced Research Projects Agency
under Electronic Systems Division Contract AF 19(628)-5167 by

Lincoln Laboratory
MASSACHUSETTS INSTITUTE OF TECHNOLOGY
Lexington, Massachusetts

The work reported in this document was performed at Lincoln Laboratory, a center for research operated by Massachusetts Institute of Technology. This research is a part of Project Vela Uniform, which is sponsored by the U.S. Advanced Research Projects Agency of the Department of Defense; it is supported by ARPA under Air Force Contract AF 19(628)-5167 (ARPA Order 512).

MASSACHUSETTS INSTITUTE OF TECHNOLOGY

LINCOLN LABORATORY

INTERFEROMETRIC PHASE AND AMPLITUDE FLUCTUATION MEASUREMENTS OVER A 7-KM ATMOSPHERIC PATH

ERNST GEHRELS

Group 64

TECHNICAL NOTE 1969-28

13 MAY 1969

LEXINGTON MASSACHUSETTS

ABSTRACT

A 6328 Å laser interferometer of the Michelson type has a one-way path length of 7 km. The fringes are resolved by frequency-modulating the laser sufficiently to sweep over at least one fringe width. By correlation techniques, the resulting fringe intensity pattern is resolved into the true fringe crossing direction and rate and into light amplitude fluctuations. An upper limit of 300 per second is established for the former, the amplitude fluctuations being at a slower rate. With a measured intensity range of up to 5000:1, it is clear from the data that none of the currently postulated Rayleigh, log normal, or Rice distributions match the amplitude statistics over this full range. A limiting value of standard deviation for the log of the amplitude is 0.85.

Accepted for the Air Force
Franklin C. Hudson
Chief, Lincoln Laboratory Office

CONTENTS

INTERFEROMETRIC PHASE AND AMPLITUDE FLUCTUATION MEASUREMENTS OVER A 7-KM ATMOSPHERIC PATH

I. INTRODUCTION

This experimental report discusses simultaneous measurements of amplitude and phase for visible laser light (6328 Å) propagated over a long atmospheric path. The technique, a variant on the Michelson interferometer, is unique to date in providing such long path phase measurements. It has also extended considerably the dynamic range of previous amplitude measurements, a matter of considerable interest for a theoretical understanding of the atmosphere. A brief summary of the present state of knowledge follows.

Tatarski[1] did the first theoretical treatment, acceptable in the modern sense, of the effect of atmospheric turbulence. He was aided by the existence of an atmospheric turbulence model due to Kolmogoroff and Obukhov.[2] In developing his theories, Tatarski[3] used the Rytov approximation, a variant on the Born approximation in which a power series of the logarithm of the radiation field, rather than of the field strength itself, is used in a perturbation analysis. This Rytov approximation has been the subject of much controversy as to whether it is really a substantial improvement over the Born approximation under conditions of multiple scattering. The necessary vindication or invalidation of its use must at present rest on experimental evidence; the mathematics is sufficiently complicated to preclude a conclusion on theoretical grounds.

The electric field of a plane wave propagating through a turbulent atmosphere may be written as

$$z(t) = \exp[x(t) + i\varphi(t)] \quad .$$

The theory predicts that both $x(t)$ and $\varphi(t)$ are normally distributed. We abbreviate the natural logarithm of the amplitude $A = |z|$ as χ. The same theory predicts the variance of $\ln A = \chi$ to be

$$\sigma^2 = 0.31\, C_n^2 k^{7/6} L^{11/6} \quad ,$$

where C_n is the structure constant of the atmospheric turbulence ($m^{-2/3}$), k is the wavenumber of the radiation (m^{-1}), and L is the optical path length

through the atmosphere (m). Another comparatively simple relation from the Tatarski theory is[4]

$$D(\rho) = D_A(\rho) + D_S(\rho) = 2.91\ k^2 L C_n^2 \rho^{5/3} \quad ,$$

where $D_A(\rho)$ is the amplitude structure fluctuation for a spacing ρ, and $D_S(\rho)$ is the phase structure function for a spacing ρ. Without going into the details of the meaning of $D_A(\rho)$ and $D_S(\rho)$, it suffices here to say that $D(\rho)$ represents the mean square of magnitude of the difference between the complex quantities $[\chi(r) + i\varphi(r)]$ and $[\chi(r') + i\varphi(r')]$, where $|r' - r| = \rho$, and $\varphi(r)$ and $\varphi(r')$ are the phase angles of the observed radiated field at the respective positions r and r'.[5] This second relation was used by Fried[6] to predict theoretically the spectral spreading and usable aperture.

Early measurements were made by Tatarski[7] and others[8,9] to determine experimentally the laws of amplitude fluctuation. Confirmation appeared to be achieved of both the predicted distance dependence of σ and of the normal distribution of χ, i.e., the log normal distribution of amplitude. There were several objections to these experiments, the most important being that either the receiver or the light source size exceeded the Fresnel zone size $\sqrt{\lambda L}$. This means that several independent light paths existed from different parts of the source to the receiver, and amplitude fluctuations appeared artificially small because of the averaging of the fluctuations between these paths.

In 1963, Gracheva and Gurvich[10] made a very careful set of amplitude measurements, obtaining simultaneous measurements of the meteorological conditions, including wind shear, to permit normalization of their results against theoretical values of the structure constant, C_n. For short distances, where the value of σ should be small, agreement was excellent; however, a saturation of σ was observed for values of σ exceeding 0.8 (incorrectly shown as 1.6, as pointed out by deWolf[11]). This result is definitely at variance with the theory using the Rytov approximation, and indicates a serious limitation of its validity at longer distances (several kilometers in the daytime). A subsequent article by Gracheva[12] reconfirms the earlier results giving, however, the correct saturation value of $\sigma = 0.8$.

The results of Gracheva and Gurvich appeared to confirm the prediction of log normal statistics, even at distances where the magnitude of σ deviates greatly from the predicted. However, deWolf[11] points out that the log normal distribution in the saturation region of 0.75 or 0.8 does not differ greatly from a Rayleigh distribution. This is particularly so when one considers that the ratio of maximum to minimum amplitude A used by Gracheva and Gurvich was 7.5:1 (intensity ratio 60:1). These same data were replotted by deWolf against a Rayleigh distribution and he obtained an equally good fit. Some of the difficulties in achieving reliable amplitude data over a wide dynamic range have been overcome in obtaining the results reported here.

The history of phase measurements is more sparse. Direct phase measurements through the atmosphere, except over laboratory distances, do not exist. There are several reasons for this, the most important being the high degree of laser stability required. Previous interferometer or coherent optical measurements over 1-km or greater path lengths were really measurements of laser stability.[13,14,15]

What has received more attention is the atmospherically induced "warping" of the wavefront, i.e., the phase difference measured at two or more closely spaced lateral points after a collimated beam has traversed a long atmospheric path. Measurements of the degradation of the image quality observed by a telescope looking through an atmospheric path are indirectly a measure of this. The most systematic set of measurements of this kind, in terms of the image modulation transfer function, was made by Coulman.[16]

An up-to-date survey of theoretical and experimental work in this field has been presented recently by Strohbehn.[17]

II. OPTICAL ARRANGEMENT

A Michelson interferometer at 6328 Å was operated over path lengths of 1.5 and 7 km to measure, among other things, the stability of optical interference "fringes" after the light had traveled through the atmosphere over round-trip path lengths of 3 and 14 km, respectively.

Figure 1 shows the interferometer optical configuration. The optical paths chosen for this experiment have an average elevation above the ground of about

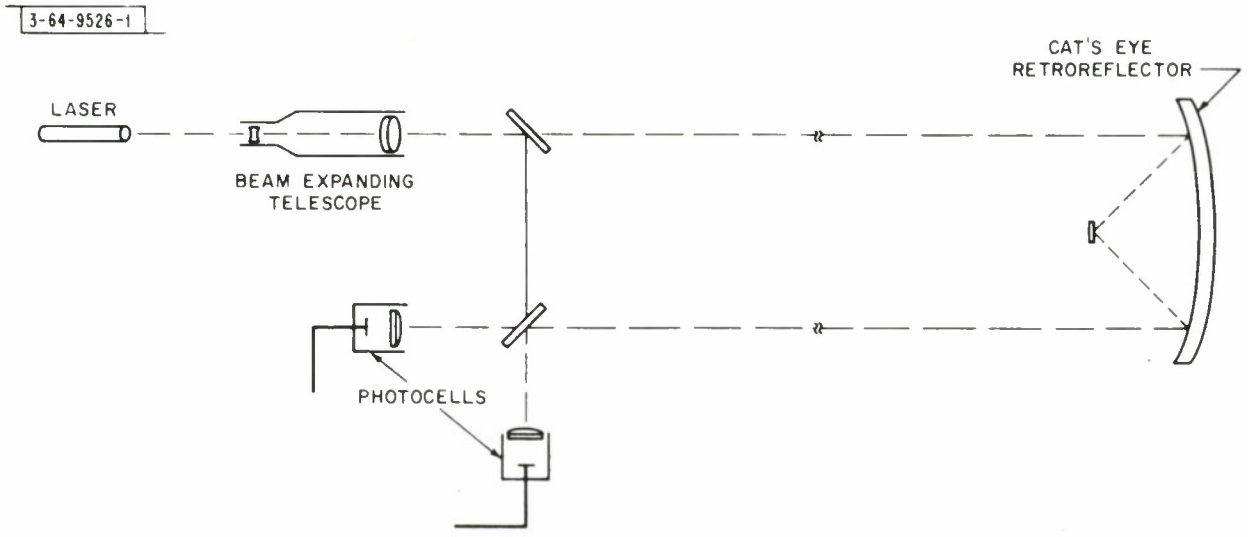

Fig. 1. Michelson interferometer, two-beamsplitter modification.

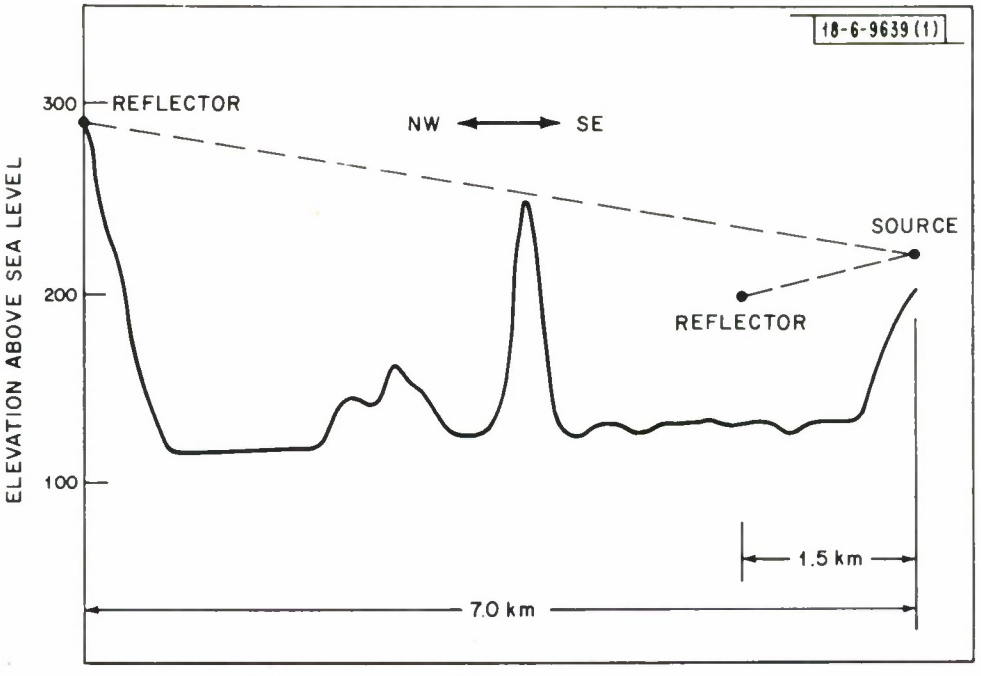

Fig. 2. Elevation profile of 1.5- and 7-km laser interferometer paths.

30 meters. Figure 2 shows an elevation profile of both paths. The main optical components are located in the Lincoln Laboratory buildings in Lexington, Massachusetts. The remote end of the 1.5-km path is a corner cube reflector located atop one of the hangar buildings at L. G. Hanscom Field in Bedford. The 7-km path represents an almost direct extension of the shorter path, crossing the airfield and the Concord River to a point near the top of Punketasset Hill in Concord. A 150-mm cat's eye retroreflector is mounted there in a box supported 4 feet off the ground.

The outgoing laser beam was intentionally allowed to spread at a sufficiently wide angle (160 μ rad) so that only a small portion of it actually impinged on the remote reflector. The beam was made this wide so that atmosphere refraction would not swing the laser beam completely off the target. One must, of course, accept the loss of light energy, which places a greater burden on the sensitivity of the photodetection system.

The return reflection from an ideal retroreflector should follow precisely the correct path back through the same atmosphere to the laser source no matter how narrow the beam collimation (theoretically, 5 μ rad from a 150-mm or 6-inch reflector at this wavelength). In reality, the beam spread of the retroreflector was observed to be more nearly 130 μ rad, even under the quietest of nighttime conditions, apparently because of misadjustment of the spacing of the optical elements within the cat's eye.

The diameter of the reference beam in the interferometer was 4.5 mm, which determines the effective aperture of the useful returned energy that enters the photodetector. The ratio of 6328 Å to this diameter determines the acceptance angle of the interferometer – in this case, 160 μ rad. Were the diameter made much larger, it would be necessary continuously to readjust the beamsplitter to follow the fluctuations of the angle of arrival of the returned light refracted by the atmosphere.

The interferometer differs from the textbook Michelson configuration in that the outgoing and return paths are displaced laterally (by about 4 cm) and in the use of two photocells at the two alternate locations where interference will occur. This use of two photocells connected in phase opposition with the proper balancing of gains permits first-order cancellation of the spurious

signal resulting from amplitude modulation of the laser. It should also be possible with this configuration to achieve a cancellation of ambient light pickup; however, advantage was not taken of this possibility. The use of a local reference much stronger than the reflected remote signal is now recognized[18] as optimum for minimizing the effect of photocell dark current noise. In this case, it permitted the use of semiconductor photodiodes instead of sensitive photomultipliers, even though the average returned optical power was on the order of 10^{-12} watts.

A procedure analogous to light chopping was employed to permit separating the small intensity fluctuation of the received interferometer beam resulting from constructive and destructive interference from the much larger intensity local reference beam and the ambient external radiation. The frequency of the laser was sinusoidally modulated (by ±50 kHz for a 1.5-km path, and by ±10.75 kHz for a 7-km path) to cause a shift of $\pm\frac{1}{2}$ fringe every 0.4 msec. Since this modulation or dithering occurs over a whole fringe width, it is also possible to observe the direction or sense of fringe movement with a single photocell (as discussed in the Appendix), provided that the fringe movement is slow with respect to 0.4 msec.

III. DATA PROCESSING

Coherent optical detection is accomplished by using the outputs of a pair of silicon photodiodes followed by field effect transistor preamplifiers in the same housings. The outputs of the photocells are processed in analog equipment to extract the optical phase and amplitudes of the return radiation from the dithered signal. The mathematics of this extraction process is given in the Appendix, and is analogous to the use of a lock-in amplifier to extract the intensity of a chopped beam in a simple incoherent amplitude measurement.

If we consider a laser output $e^{i\omega_o t}$, the returned radiation may be expressed as $z(t) = A(t) \exp\{i[\omega_o t + \varphi(t)]\}$. The two correlation detectors discussed in the Appendix produce outputs

$$x(t) = A(t) \cos \varphi(t) \quad ,$$

$$y(t) = A(t) \sin \varphi(t) \quad .$$

These two outputs are smoothed in low-pass filters of 1-msec time constant prior to being sampled at 0.4-msec intervals, i.e., at 2500 times per second. The sampled values are stored on magnetic tape to 14 bits of accuracy for further processing. From x(t) and y(t) one can compute other quantities for further analysis, for example,

$$u(t) = \cos\varphi(t) = \frac{x}{(x^2 + y^2)^{\frac{1}{2}}} \quad ,$$

$$v(t) = \sin\varphi(t) = \frac{y}{(x^2 + y^2)^{\frac{1}{2}}} \quad .$$

The amplitude is

$$A(t) = (x^2 + y^2)^{\frac{1}{2}} \quad .$$

Recovery of a useful phase angle $\Theta(t)$ is more difficult because of the ambiguity in its meaning as its variation exceeds 2π. The raw phase angle assigned over a range of just 2π can be defined as

$$\varphi(t) = \arctan\frac{y(t)}{x(t)} \quad ,$$

with a quadrant for φ being assigned on the basis of the signs of x and y. However, many of the theories describing fluctuation of coherent light, e.g., that the phase is Gaussianly distributed, are based on the assumption that the phase has a value that is unique and is not confined to the range $-\pi$ to $+\pi$. It is, of course, possible to follow the phase from time sample to time sample, relying on the fact that the phase should not change discontinuously through an angle exceeding π. One then selects the appropriate multiple of 2π that is consistent with the raw phase angle and with a change of less than π from the preceding measurement. This procedure is uncertain, particularly in a deep fade, and one must assume an expected random error of π to such an extrapolation procedure each time such a fade or dropout occurs. Such errors add up in a random walk manner over a period of time, that is, in proportion to the square root of the number of dropouts. The computer program processing for cumulative phase treated dropouts in this manner, assigning a $\frac{1}{2}$ probability of a phase advance of π and $\frac{1}{2}$ probability of a phase loss of π.

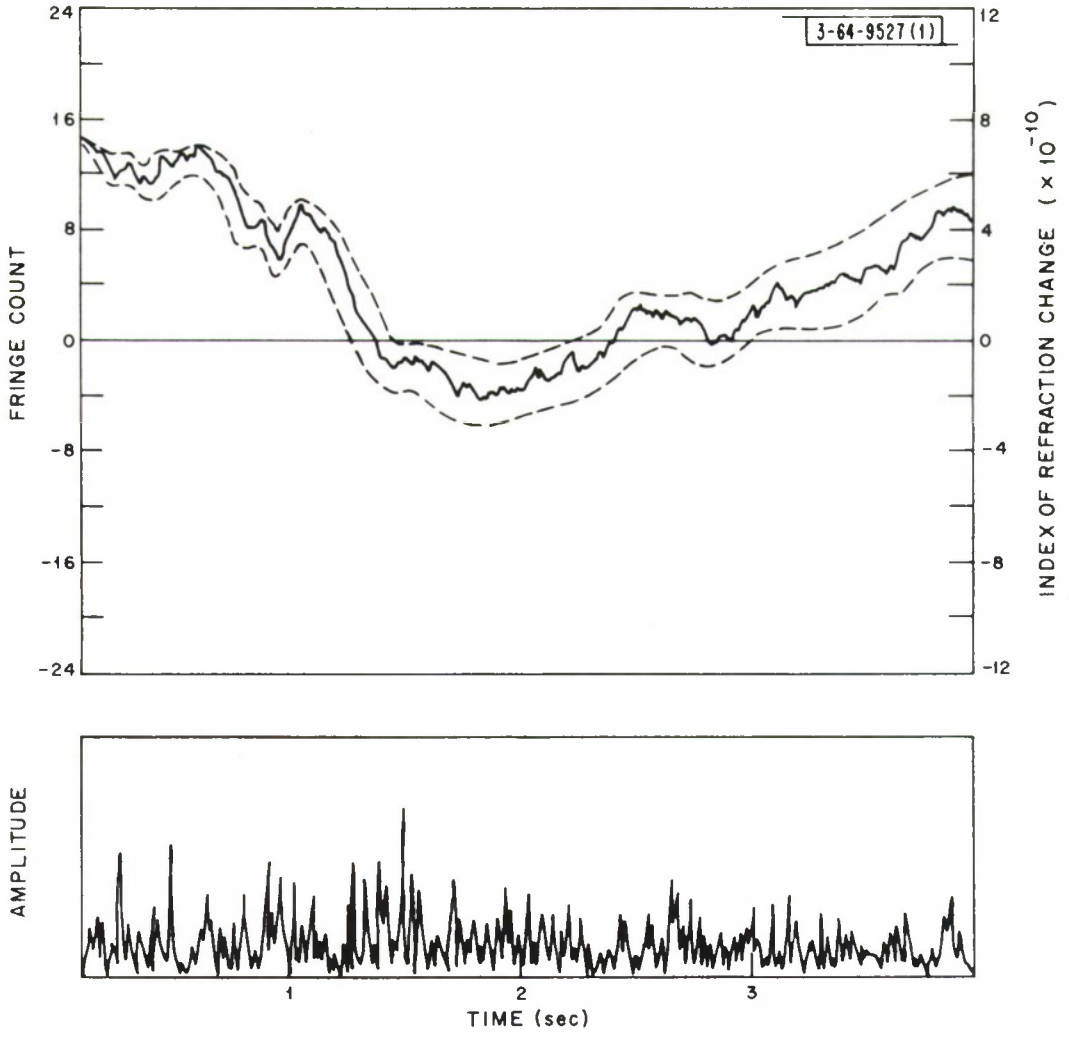

Fig. 3. Phase and amplitude for 29 July 1968 (1833 EST). Dashed curves show roughly the limits of expected phase error as a result of fades.

IV. PHASE DATA

A representative cumulative phase plot is shown in Fig. 3. Also shown by dashed lines are the expected statistical limits of error based upon the assumption of one fade every 0.05 second sufficiently deep to require a random choice of the direction of phase rotation. This fading rate is based on observed fading spectra to be discussed shortly. Over a minute's duration the cumulative phase change is typically 1000 revolutions, corresponding to a refractive index change of 1.5×10^{-8}. An expected rms error of ±18 revolutions can be attributed to the randomness of the extrapolation through dropouts of the light intensity over the 1-minute interval. Thus, the dropouts do not introduce a large uncertainty for 1-minute observations; however, for much longer intervals such as hours, the cumulative random errors, which increase as the square root of the time interval, may be expected to dominate.

In order to be confident of the data in Fig. 3, it was necessary to examine systematic errors of the system, which could be physical changes in the path length or changes in laser frequency. The former is extremely improbable, requiring either that the granite slab on which the interferometer components were mounted or the remote reflector moved 0.3 mm in a minute's time. The laser frequency stability as a substantial source of error is more difficult to discount. For short-term stability requirements, the laser had to be operated without its built-in oven or its Lamb dip stabilization, since both of these artifices, although providing long-term stability, produce fluctuations in the short-term stability. Consequently, a test was performed by comparing the laser used in the interferometer (a stabilized single-frequency laser) against a different unit very similar in manufacturer's specifications. Figure 4 shows a typical laser stability run obtained from beating two similar lasers together. Assuming the worst case of all, the instability being attributed to the laser used in the main experiment (the still worse case that the two lasers would drift together over repeated observations being very unlikely), we see a drift in frequency of 3×10^{-9} in 40 seconds.

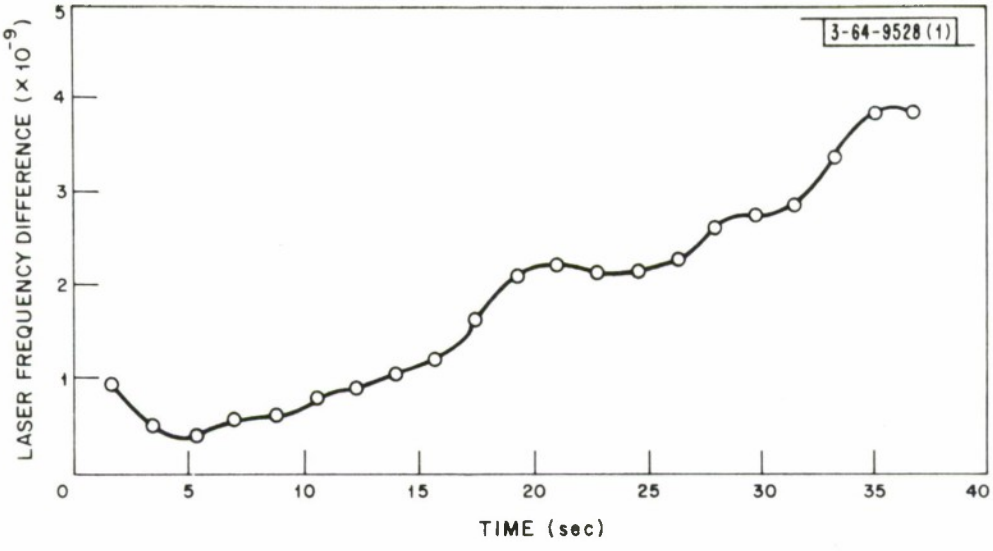

Fig. 4. Laser drift from heterodyning experiment between two lasers.

The observed magnitude of the apparent refractive index change appears to correspond quite closely to that reported by Owens,[19] the only other set of measurements known to us in which a similar quantity over a comparable path length was observed at the required accuracy. Owens reported changes of typically 6×10^{-8} for 1 minute in the group refractive index over a 5-km atmospheric path, as measured by a light beam modulated at 3 GHz. Both Owens' observations and the observations made here must be qualified by the fact that they really represent the sum of the atmospheric and instrumental variations.

These observations represent a measurement of the effects of the outer scale of turbulence, i.e., the region exceeding L_o (typically 10 to 100 meters in the horizontal direction, 1 to 10 meters vertically) in the standard treatments of the turbulent atmosphere. Little can be said by way of comparison of the experimental results with existing theory, since there is no available theory for predicting the statistics of this region. The measurement technique, however, when applied to a wider range of conditions, should provide a valuable insight into the presently unexplored outer scale region.

The primary emphasis in the present study was given to measuring the short-term phase fluctuations, which are treatable by an extension of the theory of atmospherically induced light fluctuation due to Tatarski.[7] In particular,

Fried[6] has calculated the spectral spread in a CW laser beam traversing a turbulent atmospheric path with a known refractive index structure constant (C_n^2), wind velocity, and distance.

The solid curve of Fig. 5 is a plot of the spectrum of a 4-second segment of the in-phase component x(t) [the total returned light would be described by the phasor x(t) + iy(t)].* For comparison purposes, it was of interest to examine also the spectrum of the fluctuations of amplitude A(t). Such a spectrum for the same 4 seconds is shown dotted in Fig. 5. As might be expected, the amplitude fluctuations are more concentrated in the low-frequency region.

A third set of curves was calculated for u(t), the in-phase component normalized with respect to amplitude, to ascertain whether the spectral data on the signal x(t) was being dominated by the amplitude fluctuations and was not representative of the rapidity of the phase fluctuations. As might be expected, such a procedure of normalizing the amplitude or of "limiting" does broaden the spectrum somewhat, and also has the effect of giving increased weight to those intervals when the light intensity is low. A normalized signal spectrum is plotted as a dashed curve in Fig. 5. It is seen that the spectrum of the normalized in-phase component does fall off somewhat more slowly at the higher frequencies, but that the bandwidth for x(t) is really determined by the phase rather than the amplitude spectrum.

Table I shows the spectral spread data for all the runs that have been reduced. In certain cases, two spectral calculations have been made for two or more intervals separated by a minute or more during the same data run. The consistency in these cases is quite good, especially for the in-phase component x(t), indicating that the 4-second averaging interval does give a representative sample.

---

* It would be more correct to take the spectrum of the total signal, i.e., the complex variable z(t) = x(t) + iy(t), plotting the results for both positive and negative frequencies, were there any reason to believe that the spectrum was asymmetrical. However, the observed rate of phase rotation already presented, plus the fact that x(t) and y(t) have been found to show very similar amplitude and phase statistics, gives every justification to taking the simpler course of calculating the real spectrum.

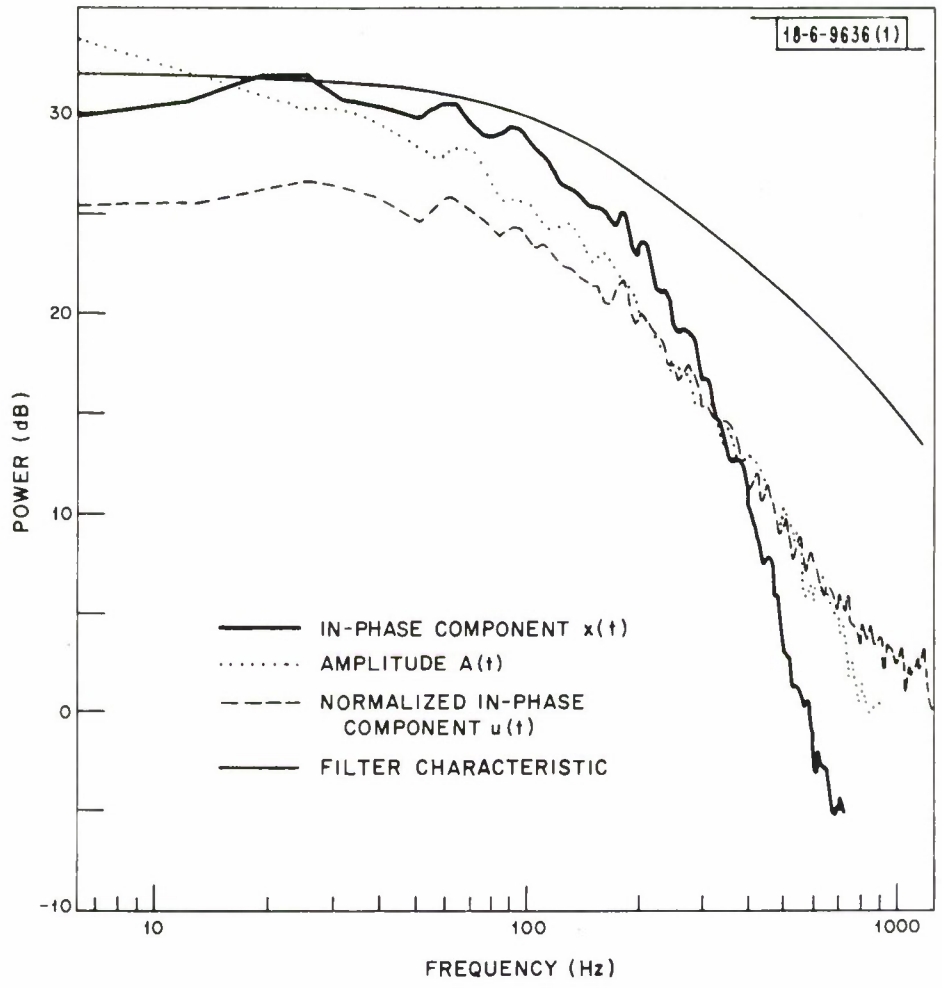

Fig. 5. Spectra of various interferometer output signals for 1 August 1968 (1317 EST).

TABLE I

COMPARISON OF THEORETICAL AND MEASURED FREQUENCY SPREAD, AND METEOROLOGICAL CONDITIONS

Date (1968)	Time (EST)	Visibility (Miles)	Temp./Dew Pt. (°F)	Wind Dir./Vel. (kt)	Crosswind Component (m/sec)	Δf_{rms} (theo.)	Δf_x (meas.)	Δf_u	Δf_A
29 July	1833	50	67/45	310°/05	0.90	28	125	220	25
29 July	2048	15	61/45	290°/05	0.0	0	210	225	17
30 July	1630	35	74/46	320°/06	1.6	35	130	130	12
31 July	1516	15	79/52	220°/10	4.9	153	325	400	160
31 July	2115	15	60/59	200°/08	4.2	131	215	350	20
1 August	1317	6 hazy	84/67	290°/10 gusts	0.0	0	265	290	35

As Table I shows, the observed spectral spreads are typically larger by at least a factor of 2 than the calculated values derived from Ref. 6, using nominal values for the unknown atmospheric parameters ($C_n^2 = 6 \times 10^{-15} m^{-2/3}$ at 35 m height, $\Delta f_{rms} = 31.2 \times v$ m/sec). Also shown in Table I are the pertinent meteorological data measured at Hanscom Field, directly astride the propagation path for these experiments. It is difficult to correlate any of the changes in spectral spread with the prevalent meteorological conditions. One reason is that all the measurements were made over a short interval of less than a week during which the weather was fairly constant. Unfortunately, no vertical temperature gradient data were available. The wind speed and direction were the most useful. The run of 31 July 1968 at 1516 EST with much higher than the usual spectral spread corresponds to a wind of 4.9 m/sec directly across the path.

The above experimental results, being relatively close in magnitude to those theoretically predicted, but not following closely the day-to-day and hour-to-hour atmospheric changes (except for the clear-cut case of very large atmospheric fluctuations on 31 July at 1516 EST) suggest that at least a portion of the phase fluctuations may be system "noise" or instability in the interferometer. Indirect measurements of the several factors contributing to possible system instability tend to confirm this on a quantitative basis, as follows.

The granite slab table on which the interferometer optics is mounted has an rms amplitude of horizontal motion of about 0.5 μm (measured by means of a horizontal short-period seismometer oriented in a NW-SE direction) resulting from vibrations on the floor of the building coupled into the system. The predominating frequency component is 16 Hz, corresponding to the resonant frequency of the shock-mounted table. This horizontal motion changes the path length and corresponds to an rms fringe-crossing rate of 200 per second, and represents one of the primary sources of instrumental noise.

As suggested previously, part of the interferometer phase fluctuation results from laser frequency instability. Several methods were employed to estimate its magnitude. A direct beating experiment between two similar lasers has already been described for estimating longer-term instability. For evaluating short-term instabilities (one second or less), more indirect methods had

to be employed since the particular comparison laser employed had very poor short-term stability as a result of a gassy plasma tube. The short-term instabilities of the laser can be ascribed to three effects: (1) mechanical motion coupled through the laser mount, (2) sound pickup by the laser, and (3) electrical modulation of the He-Ne plasma. The manufacturer gives rather detailed specifications on the sensitivity of its laser to mechanical vibration. The vertical component of motion does not change the path length, but it does affect the laser frequency. From a measured vibrational amplitude of 1 μm (as observed by vertical and horizontal seismometers mounted on the same granite table), the laser frequency shift from mechanical vibration is calculated to be less than 1.3 parts in 10^{10} or 7×10^{4} Hz. This seems like a large shift; however, as will be discussed shortly, the fact that it occurs at a slow modulation rate greatly diminishes its importance.

We obtained an approximate upper limit for acoustical frequency instability by artificially raising the room noise level by more than 40 dB, at which point a shift of 3×10^{-11} was observed directly on the interferometer. Under the usual operating conditions with all doors closed and the air conditioner momentarily turned off, the frequency shift would be in the range of 3×10^{-13} or 150 Hz.

Electrical effects, both power supply ripple and plasma noise or oscillations, affect the laser frequency by varying the gain of the lasing plasma. The primary effect, however, is to modulate the amplitude of the laser, the frequency modulation being a by-product of the latter. Again, as with the measurement of the acoustical coupling, the approach was to introduce modulation artificially, in this case by using a power supply with large ripple. A 4 percent amplitude ripple caused a readily observable 3×10^{-10} frequency shift. The degree of amplitude modulation normally present (including noise-like modulation) was 1/800 this value. All indications are that the degree of frequency modulation is linear with the degree of amplitude modulation; hence, one would expect 4×10^{-13} or a 200-Hz frequency shift from this source.

Actually, the interferometer does not observe the total spectral spread from each of these three sources, but rather the fringe crossing rate. This is the instantaneous difference in the frequency of the light leaving the laser at a time t, and light that left the laser at a time $t - \tau$, and underwent a round-trip travel time τ.

One can show that, for modulation confined to frequencies well below $f_\tau = 1/(2\pi\tau)$, the fringe crossing rate (rms) is equal to the laser frequency spread (rms) times the average modulating frequency (in the noise bandwidth sense) divided by f_τ. For the 7-km (one-way) path, f_τ = 3400 Hz; for the 1.5-km path, f_τ = 16 kHz.

From the above, the contribution from the 120-Hz ripple should amount to 18 Hz and that from the mechanical coupling to the laser (concentrated below a 20-Hz modulating frequency) should amount to 350 Hz. The acoustic coupling, covering the usual audio range, probably represents nearly a full 150/second contribution to the rms fringe crossing rate. At times of high noise level as, for instance, with an airplane flying overhead, the effect was obvious on the interferometer and the data had to be discarded.

Since several measurements of Δf_x of the path given in Table I are less than the calculated instrumental noise effects, it is the author's feeling that the latter estimates are high, partly due to overly conservative manufacturer's specifications on vibration. It is safest to simply regard the Δf_x and Δf_u figures in Table I as upper limits on the atmospheric spreading.

A quantitative examination of possible instrumental contributions to Δf_A has not been made, although it is thought that passage of the received signal with its small phase fluctuations through the limited-bandwidth receiving system might produce such fluctuations. Therefore, as with Δf_x and Δf_u, the figures for Δf_A in Table I are to be considered upper bounds on the atmospheric component.

V. AMPLITUDE DATA

The statistics of the amplitude fluctuations over an extended light path has been a subject of study for a decade, and in this experiment is a by-product. However, the coherent optical techniques used in this experiment offer two distinct advantages over the previous technique. The signal resulting from coherent or heterodyne detection, as used in the interferometer, is linear with respect to the amplitude or E vector rather than with respect to the intensity or power. This means a squaring of the dynamic range with respect to the system following the photodetector, e.g., a 100:1 voltage ratio represents a 100:1 intensity ratio in an incoherent detection system; it represents a 10,000:1 intensity

ratio in a coherent system. Also, the aperture of the light source and of the photodetector are by necessity small (4.5 mm), avoiding at the detector end the problems of aperture averaging prevalent in many of the experiments.[7]

On the debit side, this experiment uses a round-trip optical path, and the theory has not been worked out carefully for such a situation. The remote reflecting mirror system (cat's eye), however, is 15 cm in diameter and thus, being larger than the Fresnel zone size (6 cm), leads to aperture averaging at the reflector end of the path. Furthermore, the round-trip light loss is by necessity greater than a one-way light loss using similar elements; however, the over-all margin of light intensity achieved in this experiment appears to be comparable to or better than that of previous experiments.[10,12]

The amplitude data are best presented by plotting its natural logarithm, χ, on probability paper. We define the probability density of the log of the amplitude $p(\chi)$, and the cumulative probability $P(\chi)$, related by the equation $p(\chi) = (d/d\chi)\, P(\chi)$. Defining the normal integral $\Phi(\chi) = \int_{-\infty}^{\chi} \exp[-t^2/2]\, dt$, we wish to plot χ against $\Phi^{-1}[P(\chi)]$. If the amplitude is truly log normal, its natural logarithm χ will be normally distributed with a variance σ^2. This plotting procedure will yield a straight line with a slope equal to this standard deviation σ.

Figure 6 is such a plot for the run of 31 July 1968 at 1516 EST. The straight line superimposed on the data corresponds to a log normal distribution with standard deviation 0.85. Over a range of 160 in intensity, or 22 dB of dynamic range, the experimental intensities coincide within ±0.5 dB of this curve. For levels below the median intensity level, the data coincide very closely with another curve shown, the theoretical Rayleigh distribution, which has been checked experimentally using system noise only. The maximum range of validity of the experimental data is defined by two limits – the upper one due to equipment saturation, the lower one due to system noise. The left-hand vertical line indicates the rms value of the system noise, as measured by interrupting the outgoing laser beam. The right-hand vertical line is system saturation, as verified by making successive recordings at different pre-amplifier gain settings. Between these limits is a range of 37 dB or 5000:1 in intensity.

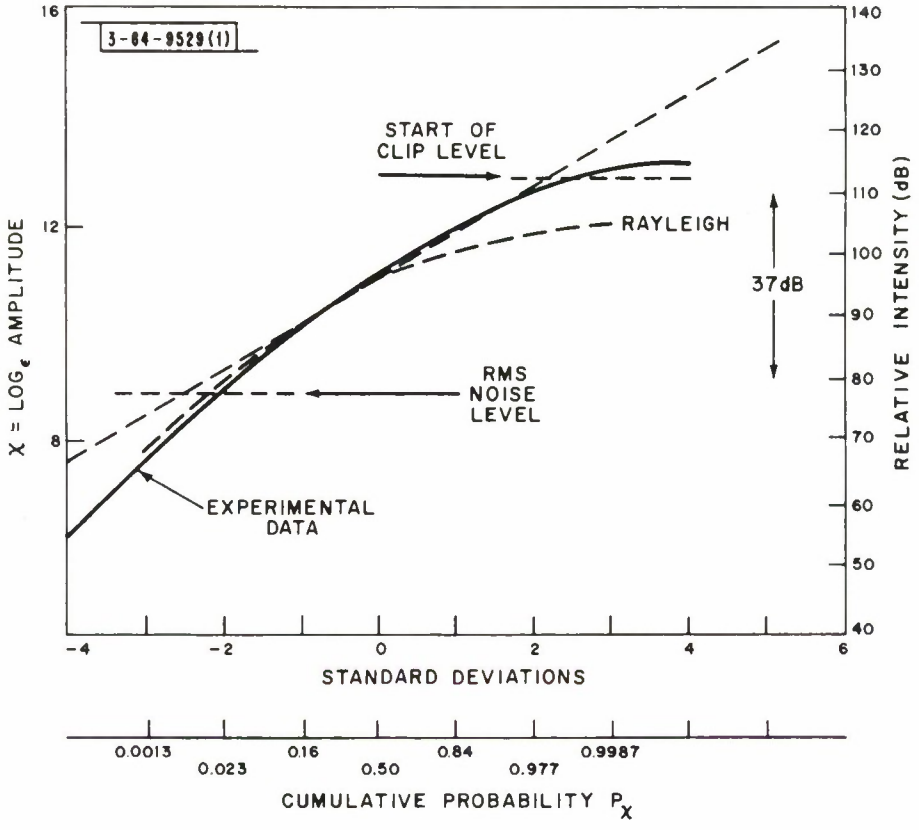

Fig. 6. Plot of log amplitude vs probability that log amplitude is less than that value for narrowband data. Abscissa is scaled according to a normal distribution. Solid line shows data of 31 July 1968 (1516 EST).

A Rice distribution has been suggested by deWolf.[20] Like the log normal distribution, the Rice distribution is a family of distributions with a normalized parameter σ. For large $\sigma \gg 1$ it approaches the Rayleigh distribution; for small $\sigma < 0.2$ it approaches the log normal with a corresponding standard deviation. No curve between these extremes would match our data.

Figure 7 shows similar plots for several other representative runs. One of the curves is for a 1.5-km optical path.

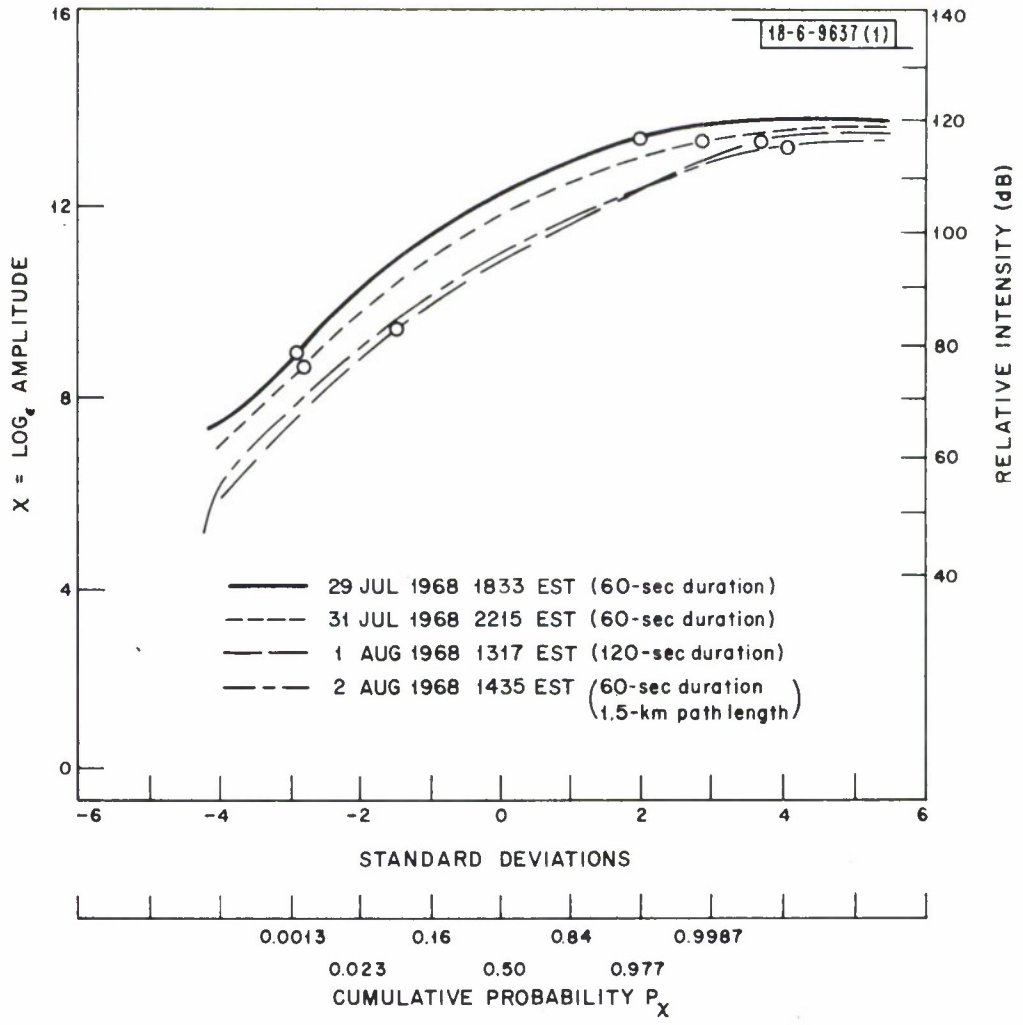

Fig. 7. Distribution plots similar to Fig. 6 for several days' data. Left points are noise level; right points are start of clip level.

The Rayleigh appearance of the data at the lower amplitudes cannot be taken at face value for two reasons. The obvious consideration is system noise, which has an independent Gaussian character on the x and y channels. The resulting distribution of the amplitude $A(t) = |x(t) + iy(t)|$ is naturally Rayleigh distributed.

Not so obvious is the effect of a limited system bandwidth. It is well known that any stationary random function subjected to a sufficiently narrowband filtering approaches a Gaussian distribution regardless of its initial distribution. The bipolar channels x and y both tend to appear more Gaussian in character and the magnitude $A(t) = |x(t) + iy(t)|$ again tends towards Rayleigh. The importance of this effect depends upon the degree of band limiting in relation to the spectral width of the actual fluctuations, but the effect will be most important at the lower amplitudes. The effect of band narrowing is to smear the amplitude record in time, i.e., a portion of the high amplitudes is smeared into subsequent low-amplitude portions, and vice versa. However, this mutual contamination represents a much greater percentage at the low amplitudes.

The more usual experiment[10,12,21] in which the output of the photomultiplier tube (which gives directly the intensity, or the square of the amplitude) suffers a somewhat different effect from band limiting. The intensity tends to assume a Gaussian distribution of non-zero mean. Again the statistical distortion is most important at low levels, the smearing tending to "fill in" the low-intensity portion of the records. This tends to bias any such measurement toward the log normal, which has a lower population than the Rayleigh distribution at very low intensities.

To avoid some of the bandwidth limitations occurring in the correlation equipment, a few of the measurements were performed directly without dithering the wavelength of the laser. The result is a simple Michelson interferometer, in which the intensity variation (above or below an average value) is the in-phase component we have represented by x(t). With this equipment simplification, we have been able to increase the bandwidth from 160 Hz to 2500 Hz.

The disadvantage of the above procedure is that the quadrature phase component y(t) is lost. The amplitude $A(t) = [x^2(t) + y^2(t)]^{\frac{1}{2}}$ is now not directly

recoverable; only the indirect relation exists, $x(t) = A(t) \cos \varphi(t)$, where the instantaneous value of $\varphi(t)$ is unknown. However, we are not interested at this point in the instantaneous value of $A(t)$, but rather in its statistical distribution.

From previous measurements, the phase was observed to go through many multiples of 2π during a single run of one minute and its value (reduced modulo 2π) should have an equal likelihood of occurring anywhere in the range $0 \leqslant \varphi < 2\pi$. Under these circumstances, we may derive the relation

$$p(\rho) = \frac{2}{\pi} \int_{\rho}^{\infty} p(\chi) \left[e^{2(\chi-\rho)} - 1\right]^{-\frac{1}{2}} d\chi \quad ,$$

where $p(\rho)$ is the probability density function of $\rho = \ln x$, and $p(\chi)$ is the probability density function of $\chi = \ln A$, as previously defined.

We may make the above integral a convolution integral with limits $-\infty$ to ∞ by defining the integrand to be zero when the quantity in brackets is negative, that is,

$$p(\rho) = \int_{-\infty}^{\infty} p(\chi)\, f(\chi - \rho)\, d\chi \quad ,$$

where

$$f(\chi - \rho) = \frac{2}{\pi} \left[e^{2(\chi-\rho)} - 1\right]^{-\frac{1}{2}} \quad , \qquad \chi - \rho > 0 \quad ,$$

$$f(\chi - \rho) = 0 \quad , \qquad \chi - \rho \leqslant 0 \quad .$$

If we express the above in terms of the Fourier transforms of the probabilities, then

$$\mathcal{F}[p(\rho)] = \mathcal{F}[p(\chi)]\ \mathcal{F}[f(\chi - \rho)] \quad .$$

We are interested in the inverse problem, solving for $p(\chi)$ from the observed density function $p(\rho)$. Using the inverse Fourier transform, the relation is

$$p(\chi) = \mathcal{F}^{-1} \left\{ \frac{\mathcal{F}[p(\rho)]}{\mathcal{F}[f(\chi - \rho)]} \right\} \quad .$$

The above computations were performed numerically on an IBM 360 computer using a Fast Fourier Transform of 2048 points for each of the variables.

Figures 8 and 9 are plots of the data for four runs processed in this manner. Also shown on Fig. 8 is a plot of theoretical Rayleigh and log normal distributions, included for comparison. The clip level appeared to be off the ordinate scale of Fig. 9.

The amplitude distribution does not follow a curve that can be described as log normal, nor as Rayleigh, nor as Rice-Nakagami. Short of claiming that a new distribution has been discovered, it is worth comparing and contrasting the distribution with the above three candidates. It will be seen that, over the 7-km path, all the curves match quite closely in slope when the log of the amplitudes is plotted on probability coordinates. This is despite the fact that the measurements were made under conditions expected to yield widely varying values of C_n, ranging from late at night to near midday on a bright summer day.

The portion of the curves below the measured noise level (indicated on each of the plots) is clearly Rayleigh, as would be expected. On the narrowband data, this Rayleigh region extends well above the noise level. The conformity is almost as good for the wideband data. It appears that for low-level excursions a Rayleigh regime prevails. This seems reasonable physically, since below average amplitudes are the result of destructive interference between two or more optical paths.

Within the intermediate range of intensities, i.e., from 1/10 to 10 times the median level, a log normal attribute can be ascribed to the distribution. In more quantitative terms, one can say that almost all the plots coincide within $\pm\frac{1}{2}$ dB over an 18-dB dynamic range (the maximum range included by Gracheva[12] in her measurements). The lower half of this region also coincides quite well with the Rayleigh curve.

It is the portion well above the median level that rules out the Rayleigh distribution. An examination shows that in all cases an intensity level 10 dB above the median level is approximately 1000 times as likely to occur in the experimental data as it would be in a Rayleigh distribution. It should be noted that any effect of equipment band limiting or of saturation would be the opposite, i.e., make the data more Rayleigh-like. A saturation effect will be noted in a curving down from the straight line of the log normal. Again, part of the effect is equipmental (clip levels are indicated in the plots); part of the effect appears to be real.

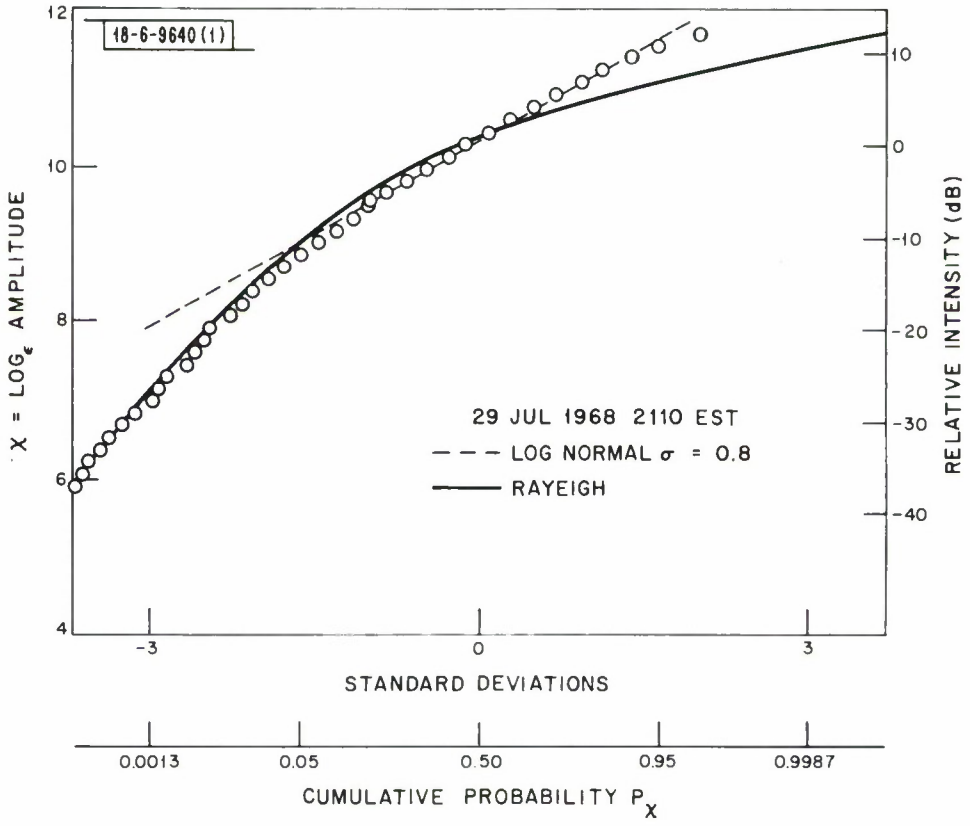

Fig. 8. Distribution plot for wideband data of 29 July 1968 (2110 EST). Also shown are two theoretical curves: log normal with $\sigma = 0.8$, and Rayleigh.

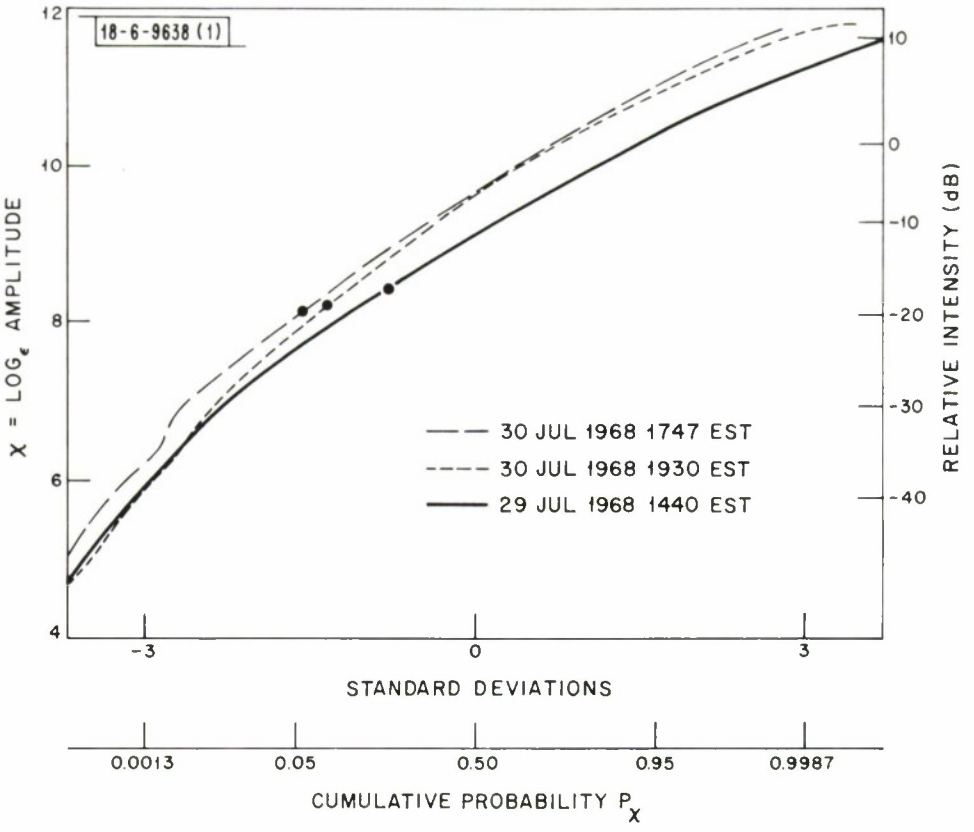

Fig. 9. Distribution plots of several days' wideband data.

VI. CONCLUSIONS

We believe that our measurements of total path phase change are the first performed over distances exceeding several hundred meters, thus giving direct optical measurements in the region of the outer scale of turbulence. Measurements in the inner scale region, namely, rapid phase fluctuations as evidenced by spectral spreading, have been made. For this region, a reasonably satisfactory theory is available, and our experimental results show agreement roughly within a factor of 2 or 3. It was not possible to ascertain that the measured phase fluctuations were solely atmospherically induced; in fact, there is good evidence that a comparable or greater amount is instrumentally induced. All the same, the measurements represent a valid upper limit (approximately 300 Hz rms half-bandwidth) to the phase fluctuations induced by atmospheric turbulence over a long path.

From the preceding, it is clear that the data fit neither a log normal nor a Rayleigh distribution. The apparent correspondence obtained by certain experimenters appears to be a result of the limited dynamic range of their apparatus. The more recently proposed Rice-Nakagami distribution predicts results differing from the experimental to an even greater extent than the Rayleigh distribution.

ACKNOWLEDGMENTS

The author appreciates valuable discussions with Charles Freed, Robert Crane, and Paul Green of this Laboratory, and also thanks Laurice Fleck and Paul Connolly for their assistance in the data processing. Special thanks go to Robert Kolker for his assistance in the field experiments.

APPENDIX

The signal processing is based on the need to obtain unambiguous phase information in the presence of variations of the intensity of the returned laser beam and of the ambient background illumination. The electrical outputs are compatible with the real-time inputs to our PDP-7 computer.

The optical path length of the interferometer is "dithered" or swept over several wavelengths at 2500 times per second.* That is,

$$\ell(t) = \ell_o + M \cos pt$$

where

ℓ = path length (optical),

ℓ_o = path length at center position of mirror,

M = amplitude of dither,

p = dither rate, $5\pi \times 10^3$ radian/second in this case,

t = time.

The intensity I, as a function of path length, is

$$I(\ell) = A(t) \cos \frac{2\pi}{\lambda} \ell + \text{const} \quad ,$$

and, as a function of time, the intensity I(t) is (disregarding the constant)

$$I(t) = A(t) \cos [\frac{2\pi}{\lambda} (\ell_o + M \cos pt)] \quad .$$

We may normalize to put the equation in a more familiar form by setting $(2\pi/\lambda)\, \ell_o = \varphi$, the phase angle for a path length ℓ_o, and $(2\pi/\lambda)\, M = m$, the phase

---

* This can be accomplished either by moving the remote mirror sinusoidally back and forth or by shifting the frequency of the laser by a small amount (about 10^4 Hz out of a carrier frequency of 5×10^{14} Hz). Although we have used the latter procedure, the discussion to follow will proceed as though the acutal mirror were moved.

modulation index introduced by the dithering of the path length, giving

$$I(t) = A(t) \cos (m \cos pt + \varphi).$$

This represents the expression for an FM signal at zero center frequency and modulation index m. What we are interested in is recovering the phase φ. This could be accomplished by cross correlating the intensity I(t) against a locally generated waveform of the same type as above and observing the value of φ that yields a maximum correlation. The same result can be accomplished by taking the cross correlation for just two values of φ: 0 and $-\pi/2$. That is, we can use two functions:

$$X(t) = \cos (m \cos pt) \quad ,$$

$$Y(t) = \sin (m \cos pt) \quad ,$$

where X(t) and Y(t) are quasi-orthogonal, approaching true orthogonality for large m. (The orthogonal interval is one period $2\pi/p$.)

Under these circumstances, if we define the cross-correlation terms,

$$x = \langle X(t)\, I(t) \rangle_{av} \quad ,$$

$$y = \langle Y(t)\, I(t) \rangle_{av} \quad ,$$

the phase angle is

$$\varphi = \arctan \frac{y}{x} \quad ,$$

where the correct quadrant assignment of φ is based on the signs of the individual quantities x and y.

It should be noted that the above analysis assumes that A(t) and ℓ_o, or φ is essentially unchanged over the time interval $2\pi/p$, corresponding to one cycle of the dither frequency. It is necessary to make this frequency sufficiently high (i.e., the time interval $2\pi/p$ sufficiently short) to ensure this. The choice of 2500 Hz appears to fulfill this requirement. This is also conveniently taken as the sampling rate for the digitized forms of x and y fed into the computer.

REFERENCES

1. V.I. Tatarski, Wave Propagation in a Turbulent Medium (McGraw-Hill, New York, 1961).
2. A.M. Obukhov, "On the Influence of Weak Atmospheric Inhomogeneities on the Propagation of Sound and Light," Izv. Akad. Nauk SSSR, Ser. Geofiz., No. 2, 155 (1953).
3. V.I. Tatarski, op. cit., Eq. (7.94).
4. Ibid., Eq. (7.98).
5. D.L. Fried, "Optical Heterodyne Detection of an Atmospherically Distorted Signal Wave Front," Proc. IEEE 55 (January 1967).
6. _____, "Atmospheric Modulation Noise in an Optical Heterodyne Receiver," IEEE J. Quant. Electron. QE-3, 213 (June 1967).
7. V.I. Tatarski, op. cit., Chap. 12.
8. A.S. Gurvich, V.I. Tatarski and L.P. Tsvang, DAN SSR 123, 33 (1958).
9. D.Y. Portman, F.C. Elder, E. Ryznar and V.E. Nobel, "Some Optical Properties of Turbulence in Stratified Flow Near the Ground," J. Geophys. Res. 67, 3223-3235 (1962).
10. M.E. Gracheva and A.S. Gurvich, "Strong Fluctuations in the Intensity of Light Propagated Through the Atmosphere Close to the Earth," Izv. Vuz. Radiofiz. 8, No. 4, 717-724 (1965).
11. D.A. deWolf, "Saturation of Irritating Fluctuations Due to Turbulent Atmosphere," J. Opt. Soc. Am. 58, 461-466 (1968).
12. M.E. Gracheva, "Research into the Statistical Properties of the Strong Fluctuation of Light when Propagated in the Lower Layer of the Atmosphere," Izv. Vuz. Radiofiz. 10, 775-787 (1965).
13. I. Goldstein, P.R. Miles and A. Chabot, "Heterodyne Measurements of Light Propagation Through Atmospheric Turbulence," Proc. IEEE 53, 1172 (September 1965).
14. W.E. Ahearn and J.W. Crowe, "Linewidth Measurement of C.W. Gallium Arsenide Lasers at 77°K," IEEE J. Quant. Electron. QE-2, No. 9 (September 1966).
15. R.B. Herrick and J. Meyer-Arndt, "Interferometry Through the Atmosphere at an Optical Path Difference of 354 m," Appl. Opt., 5, 981-983 (June 1966).
16. C.E. Coulman, "Dependence of Image Quality on Horizontal Range in a Turbulent Atmosphere," J. Opt. Soc. Am. 56, 1232-1238 (September 1966).
17. J.W. Strohbehn, "Line of Sight Wave Propagation Through the Turbulent Atmosphere," Proc. IEEE 56, 1301-1318 (August 1968).

18. A. E. Siegman, "The Antenna Properties of Optical Heterodyne Receivers," Appl. Opt. 5, 1588-1594 (October 1966).

19. J. C. Owens, "The Use of Atmospheric Dispersion in Optical Distance Measurement," paper presented at XIV General Assembly, IUGG, 25 September through 7 October 1967, Lucerne, Switzerland.

20. D. A. deWolf, "Multiple Scattering in a Random Medium," Radio Sci. 2, 1379-1392 (1967).

21. A. S. Gurvich, M. A. Kallistratova and N. S. Time, "Fluctuations of the Parameters of a Laser Light Wave Propagating in the Atmosphere," Radiophysics XI, No. 9, 1360-1370 (September 1968).

DOCUMENT CONTROL DATA - R&D

(Security classification of title, body of abstract and indexing annotation must be entered when the overall report is classified)

1. ORIGINATING ACTIVITY (Corporate author)	2a. REPORT SECURITY CLASSIFICATION
Lincoln Laboratory, M.I.T.	Unclassified
	2b. GROUP: None

3. REPORT TITLE

Interferometric Phase and Amplitude Fluctuation Measurements Over a 7-km Atmospheric Path

4. DESCRIPTIVE NOTES (Type of report and inclusive dates)

Technical Note

5. AUTHOR(S) (Last name, first name, initial)

Gehrels, Ernst

6. REPORT DATE	7a. TOTAL NO. OF PAGES	7b. NO. OF REFS
13 May 1969	36	21

8a. CONTRACT OR GRANT NO.	9a. ORIGINATOR'S REPORT NUMBER(S)
AF 19(628)-5167	Technical Note 1969-28
b. PROJECT NO. ARPA Order 512	9b. OTHER REPORT NO(S) (Any other numbers that may be assigned this report): ESD-TR-69-111
c.	
d.	

10. AVAILABILITY/LIMITATION NOTICES

This document has been approved for public release and sale; its distribution is unlimited.

11. SUPPLEMENTARY NOTES	12. SPONSORING MILITARY ACTIVITY
None	Advanced Research Projects Agency, Department of Defense

13. ABSTRACT

A 6328 Å laser interferometer of the Michelson type has a one-way path length of 7 km. The fringes are resolved by frequency-modulating the laser sufficiently to sweep over at least one fringe width. By correlation techniques, the resulting fringe intensity pattern is resolved into the true fringe crossing direction and rate and into light amplitude fluctuations. An upper limit of 300 per second is established for the former, the amplitude fluctuations being at a slower rate. With a measured intensity range of up to 5000:1, it is clear from the data that none of the currently postulated Rayleigh, log normal, or Rice distributions match the amplitude statistics over this full range. A limiting value of standard deviation for the log of the amplitude is 0.85.

14. KEY WORDS

interferometers
lasers
atmospheric turbulence
amplitude fluctuations
phase fluctuations
optical interference fringes